Vascular Smooth Muscle Sirtuin-1 Protects Against Aortic Dissection During Angiotensin II–Induced Hypertension

ORIGINAL RESEARCH

Vascular Smooth Muscle Sirtuin-1 Protects Against Aortic Dissection During Angiotensin II–Induced Hypertension

Jessica L. Fry, PhD;* Yasunaga Shiraishi, PhD;* Raphaël Turcotte, PhD; Xunjie Yu, BSc; Yuan Z. Gao, PhD; Rachid Akiki, MD; Markus Bachschmid, PhD; Yanhang Zhang, PhD; Kathleen G. Morgan, PhD; Richard A. Cohen, MD; Francesca Seta, PhD

***Background*—**Sirtuin-1 (SirT1), a nicotinamide adenine dinucleotide$^+$–dependent deacetylase, is a key enzyme in the cellular response to metabolic, inflammatory, and oxidative stresses; however, the role of endogenous SirT1 in the vasculature has not been fully elucidated. Our goal was to evaluate the role of vascular smooth muscle SirT1 in the physiological response of the aortic wall to angiotensin II, a potent hypertrophic, oxidant, and inflammatory stimulus.

***Methods and Results*—**Mice lacking SirT1 in vascular smooth muscle (ie, smooth muscle SirT1 knockout) had drastically high mortality (70%) caused by aortic dissection after angiotensin II infusion (1 mg/kg per day) but not after an equipotent dose of norepinephrine, despite comparable blood pressure increases. Smooth muscle SirT1 knockout mice did not show any abnormal aortic morphology or blood pressure compared with wild-type littermates. Nonetheless, in response to angiotensin II, aortas from smooth muscle SirT1 knockout mice had severely disorganized elastic lamellae with frequent elastin breaks, increased oxidant production, and aortic stiffness compared with angiotensin II–treated wild-type mice. Matrix metalloproteinase expression and activity were increased in the aortas of angiotensin II–treated smooth muscle SirT1 knockout mice and were prevented in mice overexpressing SirT1 in vascular smooth muscle or with use of the oxidant scavenger tempol.

***Conclusions*—**Endogenous SirT1 in aortic smooth muscle is required to maintain the structural integrity of the aortic wall in response to oxidant and inflammatory stimuli, at least in part, by suppressing oxidant-induced matrix metalloproteinase activity. SirT1 activators could potentially be a novel therapeutic approach to prevent aortic dissection and rupture in patients at risk, such as those with hypertension or genetic disorders, such as Marfan's syndrome. **(*J Am Heart Assoc*. 2015;4:e002384 doi: 10.1161/JAHA.115.002384)**

Key Words: angiotensin II • aortic dissection • sirtuin-1 • vascular smooth muscle

The walls of large arteries are composed of 3 cell types: endothelial cells, vascular smooth muscle (VSM) cells, and adventitial fibroblasts. Together with their underlying extracellular matrix, these cells form an intricate network that responds dynamically to hemodynamic changes and vasoactive factors. Among these, angiotensin II (AngII), a peptide hormone of the renin–angiotensin–aldosterone system, elicits pleiotropic effects on the vasculature. AngII is a potent vasoconstrictor signaling primarily through AngII receptor type 1 (AT1R) to constrict resistance vessels and maintain blood pressure in response to hypovolemia and increased renin. In addition, AngII can elicit inflammation and remodeling of the aortic wall via generation of reactive oxygen species (ROS), through activation of NADPH oxidases, and by production of transforming growth factor β—responses that are independent of AngII vasopressor effect on resistance vessels.[1] These combined signals produce a phenotypic switch in the media and adventitia that results in medial hypertrophy and collagen deposition, profoundly affecting the mechanical properties of the aorta.[2,3]

ROS production in the aorta is increased in aging, diabetes, and chronic inflammation—conditions associated with activation of the renin–angiotensin–aldosterone system—and it contributes significantly to the pathogenesis of aortic

From the Vascular Biology Section, Boston University Medical Campus, Boston, MA (J.L.F., Y.S., R.A., M.B., R.A.C., F.S.); Departments of Biomedical Engineering (R.T., Y.Z.G., Y.Z.) and Mechanical Engineering (X.Y., Y.Z.), and Health Science Department (Y.Z.G., K.G.M.), Boston University, Boston, MA; Advanced Microscopy Program, Center for Systems Biology and Wellman Center for Photomedicine, Massachusetts General Hospital, Harvard Medical School, Boston, MA (R.T.).

*Dr Fry and Dr Shiraishi contributed equally to this study.

Correspondence to: Francesca Seta, PhD, Vascular Biology Section, Boston University School of Medicine, 650 Albany St, X726, Boston, MA 02118. E-mail: setaf@bu.edu

Received July 7, 2015; accepted July 30, 2015.

diseases. In settings of increased endothelium-derived ROS, moderate doses of AngII (1 mg/kg per day) are sufficient to stimulate an inflammatory response in the murine aorta, which activates elastin degradation by matrix metalloproteinases (MMPs) in VSM, leading to aortic dissection.[4]

Sirtuin-1 (SirT1; mammalian homolog of silent information regulator in yeast) is a nicotinamide adenine dinucleotide$^+$–dependent deacetylase and a molecular target of polyphenols and calorie restriction.[5] SirT1 is generally associated with beneficial metabolic effects[6] by virtue of antioxidant[7,8] and anti-inflammatory[9] effects; however, the role of SirT1 in the vasculature is not fully elucidated. SirT1 deacetylates and alters the function of key molecules involved in vascular homeostasis; therefore, loss of SirT1 activity may be detrimental to the vasculature. Lack of SirT1 in VSM in apolipoprotein E–deficient mice exacerbates atherosclerosis,[10] whereas VSM SirT1–overexpressing mice are resistant to neointima formation in response to carotid artery ligation.[11] VSM SirT1 overexpression ameliorates medial hypertrophy in a model of AngII hypertension, concomitant with a decrease in inflammation, via inhibition of nuclear factor κB and transforming growth factor β.[12]

Because SirT1 is an attractive pharmaceutical target, it is crucial to elucidate the role of endogenous SirT1 and downstream signals in the vasculature. To this end, we created a mutant mouse bearing a SirT1 deletion in VSM, the major component of large elastic arteries (smooth muscle SirT1 knockout [SMKO] mice). In this study, we report that lack of VSM SirT1 results in high incidence of aortic dissection in response to AngII-induced hypertension. SMKO mice have baseline and blood pressure responses to α-adrenergic agonists comparable to wild-type (WT) littermates, and during a short course of AngII (1 mg/kg per day), they become hypertensive, although to a lesser extent than their WT counterparts. At baseline, vessel walls lacking SirT1 in VSM have normal elastin structure and aortic compliance; however, they display severely deranged elastic fibers, increased MMP activity, and stiffness on exposure to AngII, and 70% of SMKO mice die of aortic dissection within 14 days. Taken together, these data demonstrate a crucial role of VSM SirT1 in the maintenance of vascular wall integrity in response to AngII and provide a unique model of aortic dissection.

Materials and Methods

VSM SMKO Mice

All animal experimental procedures were approved by the institutional animal care and use committee at Boston University Medical Campus. Floxed SirT1 mice on a C57Bl/6J genetic background in which 2 loxP sites flank SirT1 exon 4, a critical exon required for the enzyme catalytic activity, were obtained from David Sinclair at Harvard University (Cambridge, MA). Floxed SirT1^{ex4} mice were bred with a Cre-recombinase transgenic mouse in which Cre-recombinase expression is driven by the endogenous smooth muscle 22α protein (SM22α; transgelin) promoter (endogenous locus SM22α Cre Knock-In; B6.129S6 *Tagln*$^{tm2(cre)Yec}$/J; Jackson Laboratories), generating a mouse with SirT1 exon 4 deletion in VSM (SMKO). Similarly, mice overexpressing SirT1 in VSM, (SMTg), were generated by intercrossing a transgenic mouse in which the SirT1 gene is inserted downstream of the collagen type I locus and preceded by loxP sites flanking a stop codon (obtained from David Sinclair), with the SM22α-Cre male mice described above. Cre-recombinase activity in VSM cells removes the stop codon, allowing overexpression of the SirT1 gene.

To confirm the specificity of SirT1 deletion or overexpression for the VSM, we intercrossed SM22α-Cre with Tomato reporter mice (B6.Cg-*Gt[ROSA]26Sortm9[CAG-tdTomato]Hze*/J; Jackson Laboratories). A fluorescently red Tomato protein is constitutively expressed except in cells containing Cre recombinase, in which enhanced green fluorescent protein is expressed instead of red Tomato on removal of a stop codon by the Cre-recombinase activity. Mice were housed in the Boston University Laboratory Animal Science Center in 12-hour light/dark-cycle rooms and with food and water ad libidum.

AngII-Induced Hypertension

WT, SMKO, and SMTg mice aged 8 weeks were implanted subcutaneously with Alzet osmotic minipumps (model 1007D or 1002 for 1 or 2 weeks of infusion, respectively) containing 1 mg/kg per day of AngII (item A9525; Sigma-Aldrich) dissolved in 100 μL saline or 10 mg/kg per day of norepinephrine (Sigma-Aldrich) dissolved in 100 μL saline containing 1 mmol/L ascorbate.

The occurrence of deaths and/or aortic dissections and overall animal health were closely monitored and recorded during AngII or norepinephrine administration.

The development of hypertension in response to AngII or norepinephrine infusion was monitored by radiotelemetry (Data Sciences International) in conscious, freely moving WT (n=5) and SMKO (n=5) mice. Radiotelemetry hardware included the Data Exchange Matrix, PhysioTel receivers (RCP-1), and a calibrated ambient pressure reference monitor (APR-1). Implantation of the wireless transmitters was performed in sterile conditions, following the manufacturer's recommendations. Briefly, the pressure-sensing region (4 mm) of the catheter (model TA11PA-C10) was situated in the aortic arch via catheterization of the left carotid artery in

isofluorane-anesthetized mice, and the transmitter body was placed in a subcutaneous pocket in the right flank. Recordings (1 every 4 minutes, 360 recordings per mouse per day) started after complete recovery from surgery (1 to 2 weeks). Data are expressed as mean±SEM after averaging 360 recordings per day for each mouse.

Arterial Pressures and Stiffness Measured by High-Fidelity Pressure Catheters

In addition to radiotelemetry, mean arterial pressure was assessed in anesthetized WT and SMKO mice using a solid-state high-fidelity pressure catheter (Mikro-tip catheter transducers, SPR-1000; Millar Instruments) inserted in the carotid artery. Ten minutes of stable pressure waveforms were recorded at baseline and after a bolus administration of phenylephrine (0.1 μg/g of body weight), through a P10 polyurethane tapered catheter (FunnelCath; Harvard Apparatus) inserted in the right jugular vein.

Pulse wave velocity, the standard in vivo measure of arterial stiffness, was assessed by simultaneously recording blood pressure waveforms from 2 locations along the aorta. We used a dual-pressure catheter (1.4 French) interfaced with an acquisition and analysis workstation (NIHem; Cardiovascular Engineering) with 1 kHz of bandwidth and a 5-kHz sampling rate. Briefly, saline- or AngII-treated mice were deeply anesthetized with a ketamine–xylazine mixture and kept recumbent on a heated pad (38°C). ECG was acquired through needle electrodes with lead wires connected to an acquisition system (PowerLab Animal BioAmp; ADInstruments). The catheter was inserted in the left carotid artery and then gently advanced into the aorta so that the first pressure-sensing region was situated into the aortic arch (proximal location) and the second 2.5 cm distally to obtain stable pressure waveform recordings from both locations simultaneously. The foot-to-foot transit time was assessed automatically from signal-averaged proximal and distal pressure waveforms over 20-second continuous recording using the R-wave of ECG as a fiducial point and resynchronization of sequential recordings (NIHem software v. 4.99; Cardiovascular Engineering). Pulse wave velocity was then calculated by dividing the distance (2.5 cm) by the difference among the 2 arrival times (in milliseconds). A total of 21 pulse wave velocity measurements were performed as follows: 4 in WT saline-treated mice (WT/saline), 4 in SMKO saline-treated mice (SMKO/saline), 5 in WT AngII-treated mice (WT/AngII), and 8 in SMKO AngII-treated mice (SMKO/AngII). One AngII-treated WT mouse died during surgery, and 4 AngII-treated SMKO mice presented with aortic dissection at necropsy and thus were excluded from further analysis. Pressure recordings from surviving and nondissected mice (n=4 in each group) were analyzed and computed in the group average.

Mechanical Properties of the Aorta (Ex Vivo Stiffness Measurement)

Stiffness of thoracic aortas was assessed in nondissected, viable aortic rings from saline- and AngII-treated WT and SMKO mice (n=4, WT/saline; n=4, SMKO/saline; n=5, WT/AngII; n=5, SMKO/AngII). High-frequency, low-amplitude-length oscillations, which have negligible effects on the function of the aortic rings, were used to assess ex vivo stiffness, as described previously.[13]

Aortic Morphometry and Immunostaining

Adjacent thoracic aortic rings were incubated for 30 minutes in nuclear stain (NucBlue; Life Technologies) and then captured with a fluorescent microscope, together with autofluorescence of elastin lamellae (NIS-Elements software; Nikon). A total of 15 to 20 measurements of the medial thickness (distance between external and internal elastic lamina) and diameter from 3 rings for each mouse were averaged before calculating the mean of each experimental group (n=8, WT/saline; n=7, SMKO/saline; n=10, WT/AngII; n=7, SMKO/AngII).

Aortas from saline- or AngII-treated WT and SMKO mice were snap-frozen in optimal cutting temperature compound and sectioned on a cryotome at a thickness of 6 μm. To evaluate elastin, aortic sections from the aortic root to the infrarenal aorta for each mouse were stained using an elastin staining kit (Accustain Elastin Stain; Sigma-Aldrich), based on the Van Gieson methodology, and were qualitatively analyzed in a blinded fashion by Dr Josenia Tan at Boston University School of Medicine, Department of Pathology.

Multiphoton Microscopy for Label-Free Imaging of Elastin Fibers

Elastin possesses an intrinsic 2-photon fluorescence that enables label-free imaging in intact tissue.[14–16] Freshly excised aorta from saline- and AngII-treated WT and SMKO mice (n=4, WT/saline; n=4, SMKO/saline; n=5, WT/AngII; n=5, SMKO/AngII) were imaged on a custom-built multiphoton scanning microscope. Aortas were submerged in PBS on a glass slide, and a coverslip was placed on top. Spacers were present on both side of arteries to ensure they would not be deformed by the coverslip. The 2-photon autofluorescence signal from elastin was detected at 525/45 nm and generated with 65 mW of a mode-locked Ti:sapphire laser at 800 nm (Maitai-HP; Spectra-Physics). Second-harmonic generation from collagen at 400 nm (417/80 nm) was also collected. Samples were imaged at 3 locations over the length of the descending aorta. Images were recorded at every 2 μm through the arterial thickness.

Elastin images were analyzed using the Directionality plug-in in the imaging processing software FIJI (freely available at www.nih.gov). This plug-in performs a Fourier component analysis to evaluate the dispersion of the elastin signal, as described in detail elsewhere.[17,18] The dispersion represents the variation in fiber orientation; therefore, an increase in dispersion indicates a decrease in organization. Eight regions of 32×32 μm having a unique main orientation were analyzed per artery. The dispersion value, in degrees, was normalized to the amount of fiber present in the analyzed region, another output of the Directionality plug-in.

Aortic VSM Cell Isolation

Aortic VSM cells were isolated by enzymatic dissociation, as we do routinely.[19] Briefly, aortas from WT and SMKO mice were removed, flushed with cold PBS supplemented with 1% antibiotic-antimycotic (Anti-Anti; Gibco, Life Technologies), and cleaned of periaortic fat. Cleaned aortas were then washed in PBS and incubated at 37°C for 12 minutes in 3 mg/mL collagenase II (Worthington) in serum-free DMEM. Adventitia was removed manually and preserved at −80°C until Western blot or quantitative reverse transcription polymerase chain reaction (qRT-PCR), analysis. The medial layer was further dissociated in 3 mg/mL collagenase and 1 mg/mL elastase at 37°C for 30 minutes with gentle agitation every 10 minutes. Cells were centrifuged and resuspended in complete growth medium (DMEM, 1 g/L glucose supplemented with 10% FBS and 1% Anti-Anti) and used until passage 10.

Quantitative RT-PCR on Aortic Extracts

The mRNA expression of several genes of interest (SirT1 exon 4, AT1R, MMP2, MMP3, MMP9, MMP19, MYH11) in aortic and VSM extracts was assessed using standard procedures. Briefly, total RNA from aortas and VSM cells of WT and SMKO mice was extracted with Trizol (Life Technologies), followed by chloroform separation and isopropanol precipitation. After total RNA retrotranscription (High-Capacity RNA-to-cDNA Kit; Applied Biosystems, Life Technologies), RNA expression of genes of interest was analyzed by quantitative RT-PCR with verified TaqMan assays multiplexed for β-actin (AB750 instrument; Applied Biosystems). Relative mRNA quantitation was calculated by the ΔΔCt method, expressed as relative to controls and normalized by β-actin, used as an endogenous control.

VSM Cell and Aortic Lysate Immunoprecipitation and Western Blot

VSM cells from WT and SMKO mice were cultured in DMEM containing 10% FBS and 1% Anti-Anti in triplicate tissue culture–grade 10-cm dishes. VSM cells were dissolved in RIPA buffer (200 μL/1 mg tissue; Cell Signaling Technology) supplemented with protease inhibitor cocktail and trichostatin A (5 μmol/L), as appropriate. After brief sonication (10 seconds, 3×, on ice), protein concentration was assessed using the Pierce BCA Protein Assay (Thermo Scientific), per the manufacturer's instructions. For immunoprecipitation studies, equal amounts of proteins were incubated overnight at 4°C with 2 μg of an anti–acetyl lysine antibody immobilized to agarose beads (ImmunoChem) with rotating agitation. Beads were then washed with PBS and 1% NP40 3 times before elution with Laemmli buffer and Western blotting. To confirm effective deletion of active SirT1 in VSM, whole aortas or media and adventitia, separately, from saline- and AngII-treated WT and SMKO mice were manually disrupted with a glass–glass homogenizer on ice and dissolved in RIPA buffer, as described above.

VSM cell or aortic lysates and immunoprecipitated proteins were resolved by SDS-PAGE (7.5% or 4% to 20% polyacrylamide gels) and transferred to PVDF membranes (100 V, 120 minutes). Membranes were blocked in 5% nonfat milk in 1% Tween-20 in PBS (PBS-T) for 1 hour and incubated with 1 of the following antibodies overnight at 1:1000 dilution: SirT1 (item ab110304; Abcam), SM22α (a kind gift from K.G.M.), p53 (item 2524; Cell Signaling Technologies), TIMP-1 (item ab38798; Abcam), galectin-3 (item ab53082, Abcam), VCAM-1 (item 14694; Cell Signaling Technologies), and β-actin (item A5441; Sigma-Aldrich). Membranes were then washed in PBS-T and incubated with peroxidase-conjugated anti-mouse or anti-rabbit antibodies (Cell Signaling Technologies) and exposed to the chemiluminescent substrate ECL (GE Healthcare) to visualize protein bands. Protein band intensities were quantified with ImageJ (National Institutes of Health, www.nih.gov), averaging band intensities pertaining to the same experimental group.

In-Gel Zymography

Whole aortas, from the aortic root to the common iliac bifurcation, were dissected from saline- or AngII-treated WT, SMKO, or SMTg mice (n=4 in each group) and cleaned of periaortic fat. Aortas were divided into 8 equal parts and cultured at 37°C in 50 μL DMEM overnight. In a subset of experiments, freshly prepared tempol (10 mmol/L) was added to DMEM. Aortas were then homogenized on ice with 100 μL lysis buffer (50 mmol/L Tris, 10 mmol/L $CaCl_2$, 150 mmol/L NaCl, 1% Triton X-100, 0.1% SDS, 0.5% Brij 35, 0.05% azide pH 7.4) and centrifuged at 16100 g for 15 minutes to obtain the protein supernatant. Protein content of the aortic lysates was determined with the BCA Protein Assay (Thermo Scientific), per the manufacturer's instructions. Equal amounts of aortic proteins and corresponding cultured aortic medium from 4 aortic homogenates, 1 from each experimental group for a total of 8 samples, were loaded

into a 10% zymogram gel containing gelatin as MMP substrate (item 161-1167; Bio-Rad) after mixing with zymogram loading buffer (item161-0764; Bio-Rad). Protein separation was carried out in SDS-containing buffer for 5 hours at 4°C. SDS was then exchanged with Triton X-100 for 30 minutes at room temperature by soaking the gels in zymogram renaturation buffer (item161-0765; Bio-Rad), which was then replaced by the zymogram development buffer (item 161-0766; Bio-Rad) for 30 minutes at room temperature. After a second change of fresh development buffer, the gels were incubated for 2 days at 37°C and stained with 0.5% Coomassie Brilliant Blue R-250 (item 161-0400; Bio-Rad) dissolved in 40% methanol and 10% acetic acid for 1 hour. Gels were then destained with 20% methanol and 5% acetic acid. Gel images were captured by transillumination with a scanner (Perfection 4990 Photo; Epson) at 48-bit color and 300-dpi resolution. White bright bands over a blue background were indicative of gelatin in-gel digestion by the enzymatic activity of MMPs.

Oxidant Measurement by Dihydroethidine

Dihydroethidine (DHE) was used to assess oxidant levels in VSM cells and fresh frozen aortic sections. In the presence of oxidants, mainly superoxide anion, DHE is oxidized to ethidium, which intercalates with nuclear DNA generating a red fluorescent signal. DHE solution (10 mmol/L) was freshly prepared in DMSO and diluted to 10 μmol/L working solution in PBS. Tiron, a superoxide scavenger, was freshly prepared at 10 mmol/L working solution (pH 7.4) and used to confirm the specificity of DHE fluorescence signal.

Aortas from saline- or AngII-treated WT and SMKO mice were frozen in optimal cutting temperature compound and kept at −80°C until sectioning in a cryotome at a thickness of 10 μm. Aortic sections were washed on ice with cold PBS and incubated with DHE solution at 37°C for 45 minutes. A sequential section from the same aorta was positioned onto the same slide so that a tiron treatment (10 mmol/L, pH 7.4) could be run in parallel. Sections were then washed in PBS and coverslipped with Prolong Gold Antifade mounting medium (Life Technologies). Digital images were captured with an epifluorescent microscope (Nikon Eclipse 80i), a CDD camera (DQ Qi Mc), and NIS-Elements 3.22 software (Nikon) and scored for red fluorescence intensity by 4 independent observers, blinded to the experimental groups. Scores pertaining to the same experimental group were averaged (n=7, WT/saline; n=5, SMKO/saline; n=5, WT/AngII; n=12, SMKO/AngII).

VSM cells were obtained from WT and SMKO aortas, as described above, cultured in triplicate 10-cm culture dishes

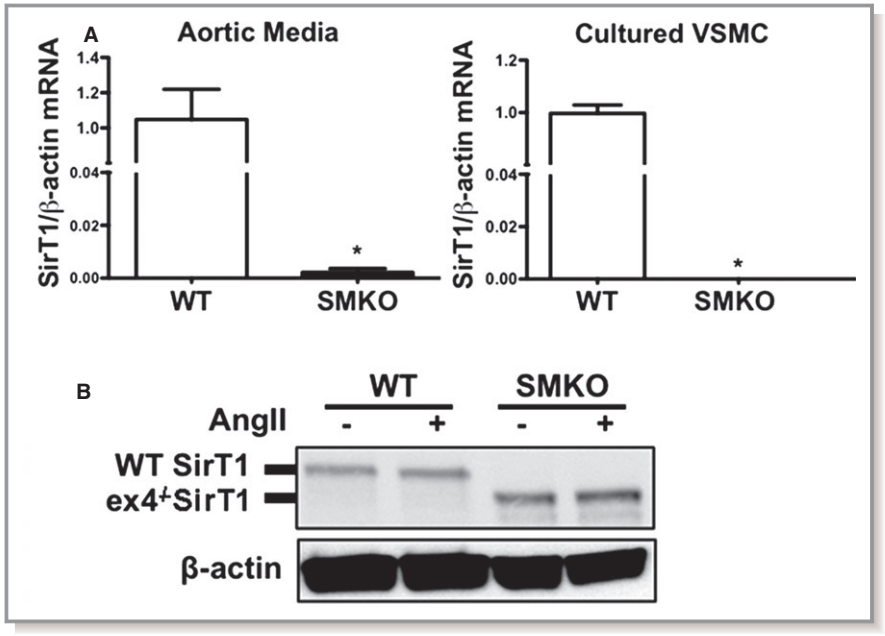

Figure 1. Novel mouse strain with SirT1 deletion in vascular smooth muscle (SMKO). A, Specific genetic deletion of VSM SirT1 exon 4 confirmed by qRT-PCR on aortas (n=5, WT and n=5, SMKO) and cultured VSM cells (n=3). SirT1 mRNA expression normalized to β-actin and expressed as fold-change vs WT. *P<0.05 vs WT. B, Representative Western blot for WT and exon $4^{-/-}$ SirT1 in aortic media from WT (n=4) and SMKO mice (n=4). Each lane represents 1 mouse. AngII indicates angiotensin II; ex, exon; qRT-PCR, quantitative reverse transcription polymerase chain reaction; SirT1, sirtuin-1; SMKO, smooth muscle SirT1 knockout; VSM, vascular smooth muscle; VSMC, vascular smooth muscle cells; WT, wild type.

to 80% confluence and serum-starved overnight before treatment with AngII (100 nmol/L, 6 hours) or vehicle (PBS) in the presence of DHE or DHE plus tiron. At the end of the treatment period, VSM cells were washed in Hanks' balanced salt solution, trypsinized, and analyzed by flow cytometry with the assistance of the Boston University Analytical Core (LSRII Flow Cytometer; BD Biosciences).

Inflammatory Cell Quantitation by Flow Cytometry

Methods for quantitation of inflammatory cells in the aorta were adapted from Moore et al.[20] Briefly, nondissected thoracic aortas from AngII-treated WT (n=5) and SMKO (n=4) mice were isolated and manually minced with fine scissors. Aortas were enzymatically digested for 40 minutes

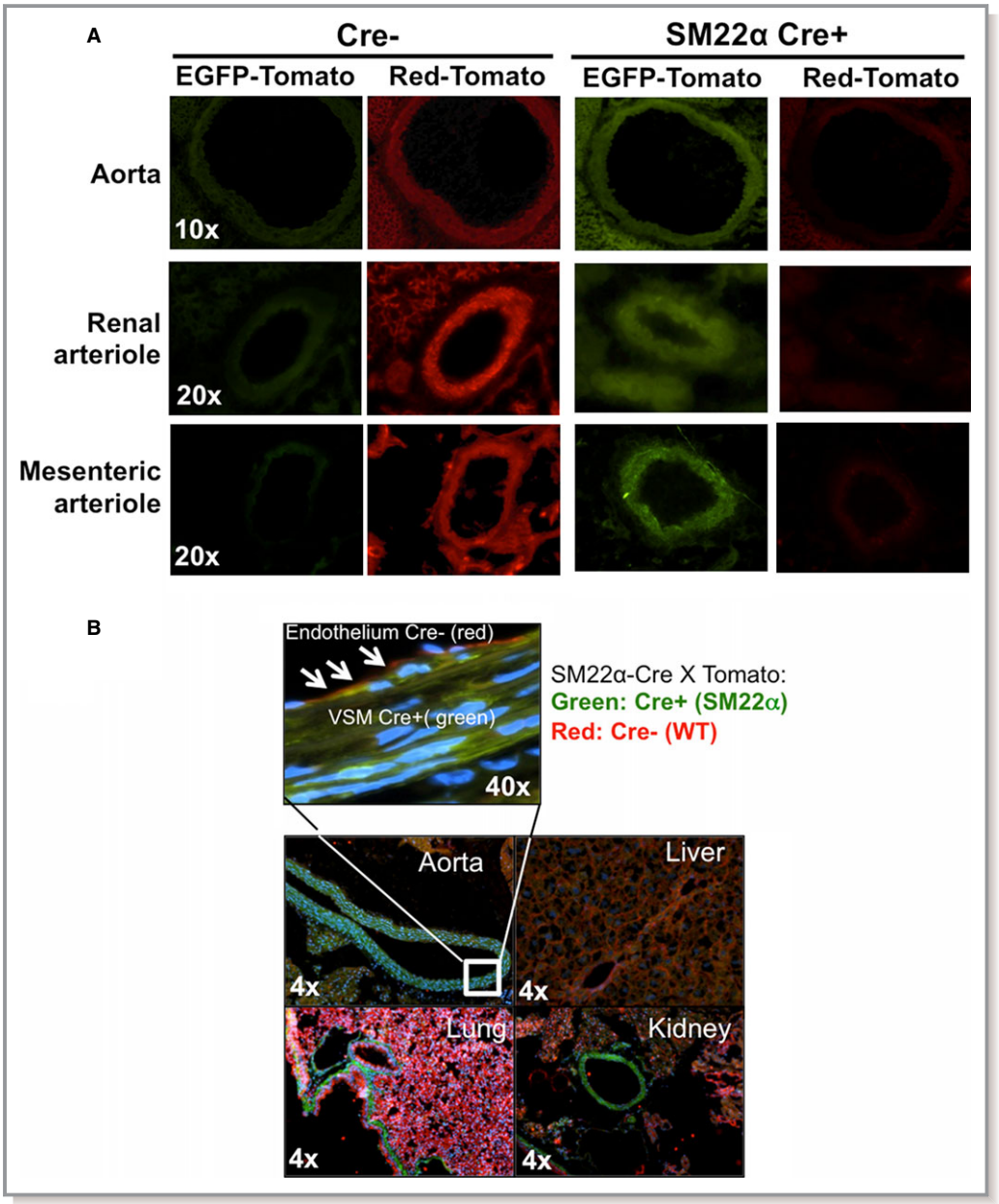

Figure 2. Specific Cre-recombinase expression in VSM. Representative pictures from tissues of a Tomato reporter mouse. A, From top to bottom: green (EGFP-Tomato) and red (Red-Tomato) fluorescence in aorta (×10), renal and mesenteric arterioles (×20) of SM22α-Cre^{-} (left) and SM22α-Cre^{+} (right) mice. B, Specific Cre-recombinase expression achieved in VSM of aorta (magnified in top panel, ×40) and arteries of indicated tissues but not in their parenchyma (×4). Red fluorescence signal indicates Cre^{-} cells and green fluorescence indicates Cre^{+} cells. EGFP indicates enhanced green fluorescent protein; SM22α, smooth muscle 22α protein; VSM, vascular smooth muscle; WT, wild type.

at 37°C under gentle agitation with a mixture of collagenases type IX and type I-S and hyaluronidase I-S dissolved in PBS containing Ca^{++} and Mg^{++}. Cell debris and undigested material were removed by passing the suspension though a 70-μm cell strainer. Subsequently, 1 million cells from each digested aorta were incubated with fluorescently conjugated CD45 and CD11b antibodies or isotype controls (Biolegend) in PBS containing 5% BSA for 25 minutes at 4°C, washed, and immediately analyzed by flow cytometry (LSRII Flow Cytometer, Boston University Flow Cytometry Core). Data are expressed as the average of percentage of $CD45^{+}CD11b^{+}$ cells from triplicate experiments.

Echocardiography to Assess Left Ventricular Function

Cardiac function of WT (n=4) and SMKO (n=5) mice aged 8 weeks was assessed by echocardiography (VisualSonics Vevo770, Toronto, Canada). Mice were lightly anesthetized with isofluorane/O_2 to keep heart rates in the range of 400 to 500 beats per minute. Left ventricular ejection fraction and fractional shortening were measured with the left ventricular wall trace measurement tool (Vevo770 v3.0 software; VisualSonics) from M-mode images acquired from a left parasternal short-axis view at the level of the papillary muscles.

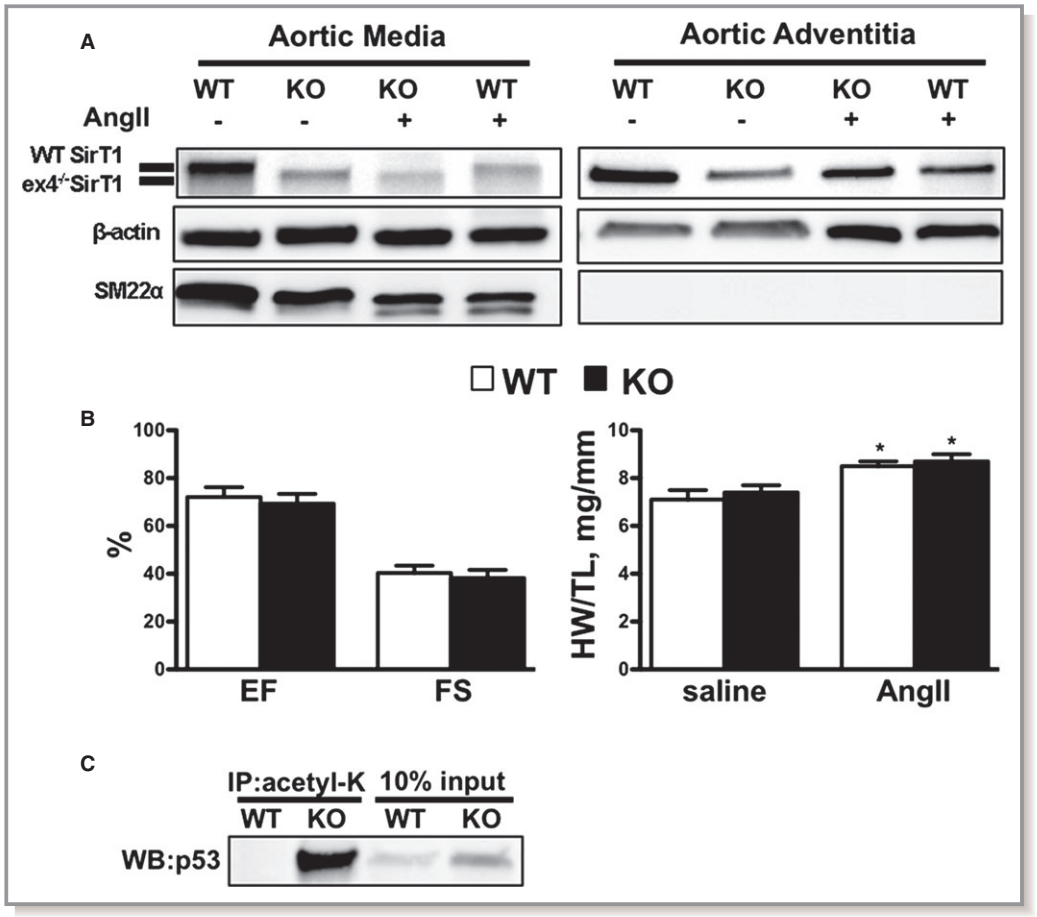

Figure 3. SirT1 deletion in SMKO is specific for the aortic media. A, Representative Western blot for WT and exon $4^{-/-}$ SirT1 in aortic media and adventitia from WT and SMKO (KO) mice. Adventitia did not express either the deleted variant (exon $4^{-/-}$ SirT1) or the smooth muscle marker SM22α before or after AngII. Each lane represents 1 mouse. n=4 for each experimental group. B, Percentages of EF and FS measured by echocardiography in lightly anesthetized WT (n=4) and SMKO mice (n=5) and HW/TL (in mg/mm) in saline- and AngII-treated WT and SMKO mice (n=4 in each group). **P*<0.05 vs saline. C, Representative image of triplicate Western blots for acetylated p53 of WT and SMKO VSM cell homogenates IP with an anti–acetyl lysine antibody, indicative of SirT1 activity. 10% input, whole cell lysates without IP. AngII indicates angiotensin II; EF, ejection fraction; Ex, exon; FS, fractional shortening; HW/TL, heart weight/tibia length ratio; IP, immunoprecipitated; K, lysine; KO, smooth muscle SirT1 knock out; SirT1, sirtuin-1; SM22α, smooth muscle 22α protein; WT, wild type.

Statistical Analysis

All data are expressed as mean±SEM and analyzed by Student *t* test or by 1-way ANOVA to compare means of controls and experimental groups. If data were not normally distributed, Kruskal–Wallis with Dunn's multiple comparisons post test was used. Repeated measures of blood pressure over time were analyzed by 1-way ANOVA with Dunnett's multiple comparisons post hoc test. Kaplan–Meier survival curves with Wilcoxon post hoc test were used to assess the mortality of mice in different experimental groups. One-sided Wilcoxon rank-sum test was used to analyze dispersion of elastin by multiphoton autofluorescence. *P* values <0.05 were considered significant.

Results

AngII-Treated VSM SMKO Mice Die of Aortic Dissection

To evaluate the role of VSM SirT1 in AngII-induced aortic remodeling, we generated a mouse with a SirT1 exon 4 deletion specifically in VSM (SMKO) and confirmed the deletion of functional SirT1 using both quantitative RT-PCR and Western blot of aortic media, adventitia, and cultured aortic VSM cells. Consistent with previous reports in other tissues,[21,22] we found that SirT1 mRNA was decreased by ≈99% in aorta of SMKO mice compared with WT mice (Figure 1A). SMKO aortic media produced a truncated SirT1 protein with an apparent molecular mass ≈7 kDa lower than WT SirT1 that lacked the functional deacetylase domain (Figure 1B). We further confirmed the deletion in smooth muscle of aorta and other vessels, but not in the parenchyma of major organs, by intercrossing SM22α-Cre with a Tomato reporter mouse (Figure 2). Adventitial fibroblasts may acquire a myofibroblast (SM22α^{+}) phenotype in response to increased aortic wall stresses because the adventitia becomes a major load-bearing component of the arterial wall under high pressures. Although the truncated SirT1 protein was not present in the adventitia of SMKO mice, we explored the possibility that, in response to AngII, SM22α^{+} myofibroblast might start expressing Cre-recombinase, resulting in SirT1 deletion in adventitia; however, neither SM22α nor the exon 4–deleted SirT1 variant were detected in the adventitia after AngII in SMKO mice, confirming the deletion for the aortic

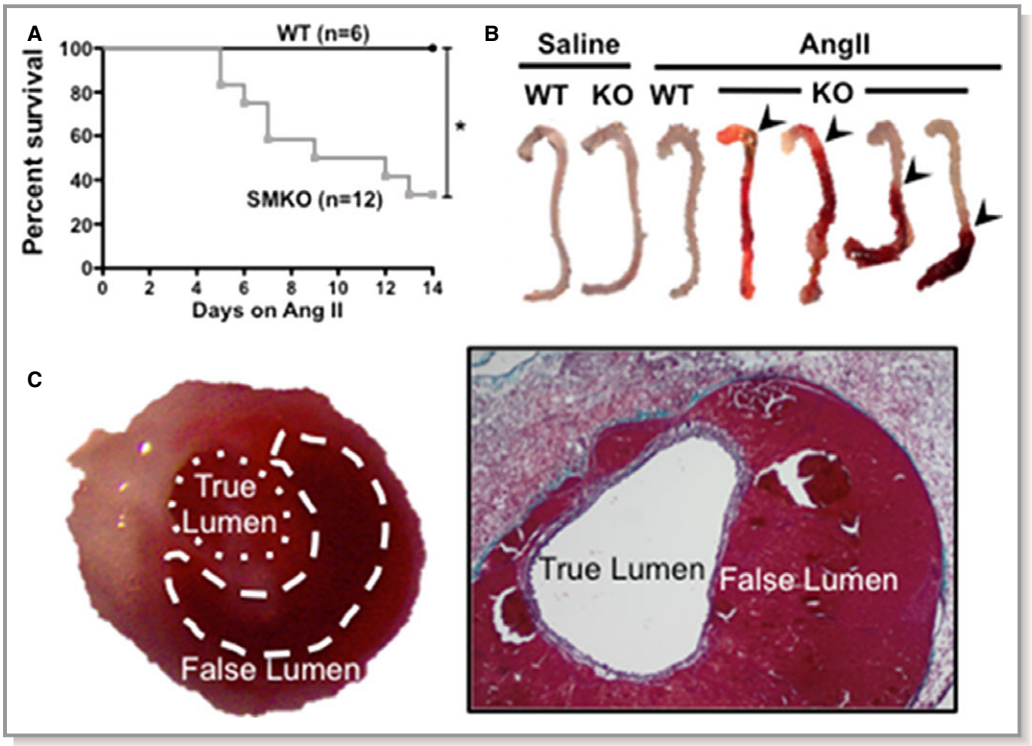

Figure 4. In response to AngII, SMKO mice die of aortic dissection. A, Survival curves of WT and SMKO (KO) mice over a 14-day course of AngII infusion. Number of mice indicated in parenthesis. **P*<0.05 vs WT. B, Representative pictures of aortas from saline- and AngII-treated WT and SMKO (KO) mice. Aortic dissections are evident in AngII-treated SMKO mice. Arrowheads indicate the point of aortic wall tearing. C, Representative pictures of a dissected aorta from an AngII-treated SMKO mouse, viewed through the longitudinal axis. True and false aortic lumens are highlighted with dashed lines (left). False lumen filled with blood, as confirmed by Masson's trichrome staining on aortic sections (×4, right). AngII indicates angiotensin II; KO, smooth muscle sirtuin-1 knockout; WT, wild type.

media (Figure 3A). In addition, although SM22α expression is restricted to smooth muscle lineage during late embryonic stages and throughout adulthood, SM22α could be expressed in cardiac myocytes during early embryogenesis.[23] SMKO mice, however, had cardiac ejection fractions and fractional shortenings (assessed by echocardiography) and heart weight/tibia length ratios (Figure 3B) and heart rates comparable to WT littermates, indicating a normal cardiac phenotype.

To confirm a decrease in SirT1 deacetylase activity in our novel mouse strain, we assessed the levels of acetylated p53, a proapoptotic transcription factor with activity inhibited by SirT1-mediated deacetylation.[21] Acetylated p53 was significantly increased in VSM cells from SMKO aortas compared with WT (Figure 3C), consistent with decreased SirT1 activity in VSM of our novel murine model.

To evaluate the role of VSM SirT1 in aortic remodeling, a hypertensive dose of AngII (1 mg/kg per day) was administered to WT and SMKO mice for 14 days using osmotic minipumps. AngII strikingly increased mortality in SMKO mice beginning as early as day 5 of treatment, with ≈50% of mice dying within 9 days and only ≈30% surviving until day 14 (Figure 4A). On necropsy, mice that spontaneously died or

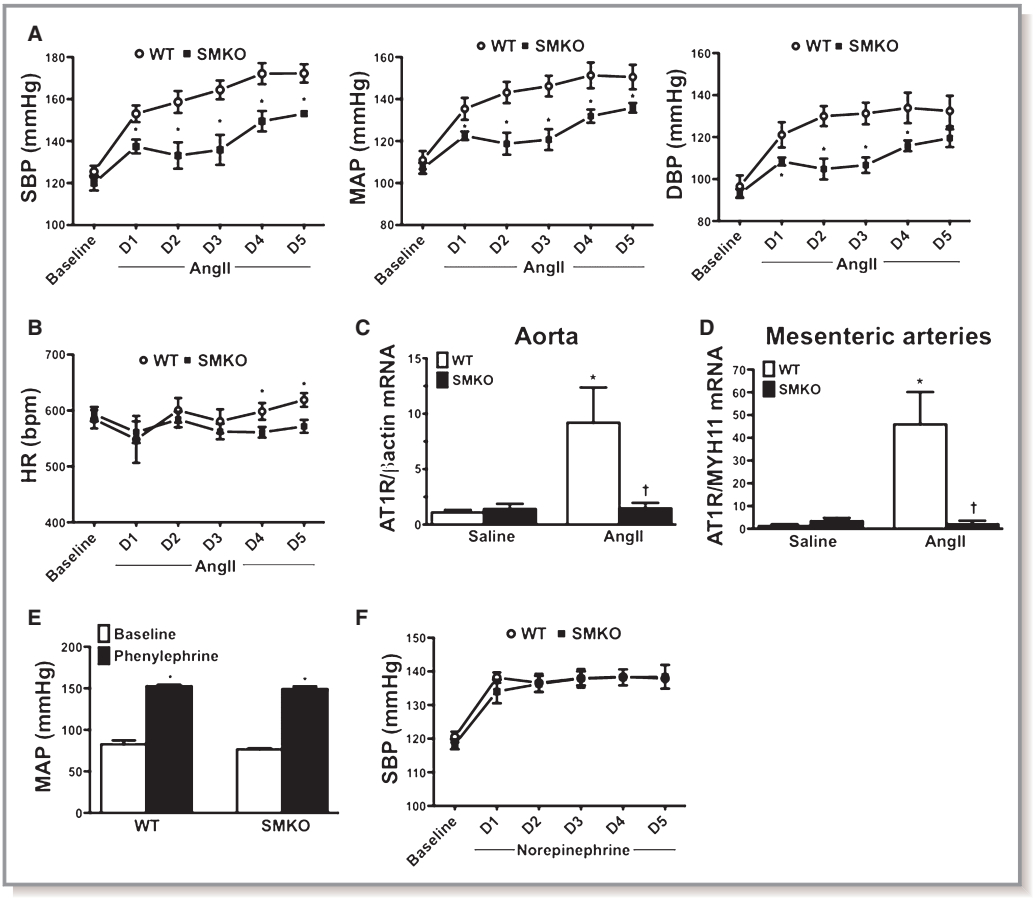

Figure 5. Vasoconstrictor responses in WT and SMKO mice. Blood pressures (A) and HRs (B) measured by radiotelemeters in conscious WT and SMKO mice before (baseline) and during 5 days (D1 to D5) of AngII infusions (1 mg/kg per day). n=5 in each group; **P*<0.05 vs WT. Quantitative RT-PCR of aortic (C) and mesenteric (D) artery mRNA extracts from saline- and AngII-treated WT and SMKO mice (n=7, WT/saline; n=8, SMKO/saline; n=9, WT/AngII; n=9 SMKO/AngII). **P*<0.05 vs WT/saline, †*P*<0.05 vs WT/AngII, by Kruskal–Wallis test with Dunn's post test. Data are normalized to endogenous β-actin and, for mesenteric arteries, expressed as ratio of the vascular smooth muscle–specific marker MYH11. E, Blood pressures measured by intra-arterial (carotid artery) pressure catheters in anesthetized WT and SMKO mice before and after an intravenous bolus of phenylephrine (100 μL, 1 mmol/L). n=4 in each group; **P*<0.05 vs baseline. F, Pressure responses to norepinephrine infusions (10 mg/kg per day) in WT and SMKO mice measured by radiotelemetry. n=4 in each group. **P*<0.05 vs WT. AngII indicates angiotensin II; AT1R, AngII receptor type 1; D, day; DBP, diastolic blood pressure; HR, heart rate; MAP, mean arterial pressure; MYH11, myosin heavy chain 11; SBP, systolic blood pressure; SMKO, smooth muscle sirtuin-1 knockout; WT, wild type.

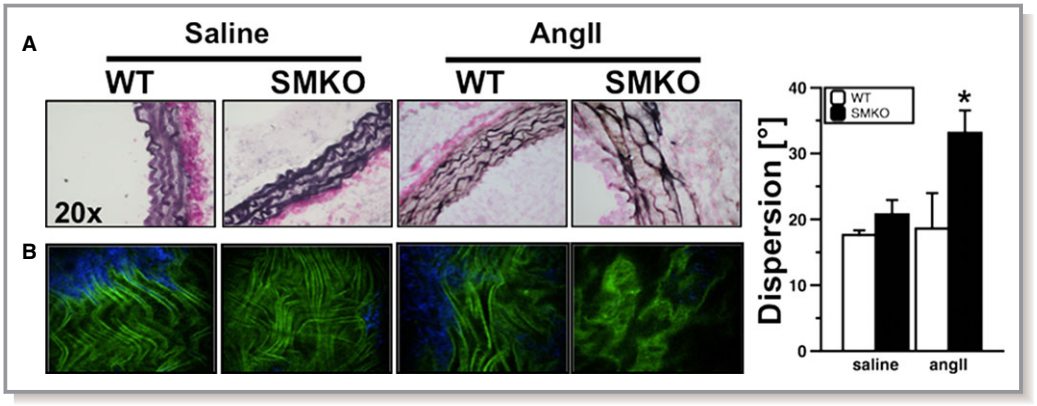

Figure 6. AngII causes elastin fragmentation in SMKO aortas. Representative pictures of elastin-stained (Van Gieson) aortic sections (×20) (A) and elastin fiber microstructure by multiphoton microscopy (green: elastin, blue: collagen; image width: 306 μm) (B) from saline- and AngII-treated WT and SMKO mice. Descending aortas are displayed. C, Quantification of elastin microstructure from saline- and AngII-treated WT and SMKO mice (1-sided Wilcoxon rank-sum test, **P*<0.05 vs WT/AngII; n=4, WT/saline; n=4, SMKO/saline; n=5, WT/AngII; n=5, SMKO/AngII) based on the elastin fiber dispersion in the descending aorta. AngII indicates angiotensin II; SMKO, smooth muscle SirT1 knockout; WT, wild type.

required euthanasia had blood in either the thoracic or abdominal cavity. Thrombosis was evident in the aortic wall in the thoracic or abdominal region and, in some cases, in both regions (Figure 4B and 4C).

Considering that hypertension is a major risk factor for an aortic dissection,[24] we determined whether SMKO mice had an exaggerated hypertensive response to AngII by monitoring the development of AngII-induced hypertension with radiotelemeters. Although WT and SMKO mice have similar baseline systolic, mean, and diastolic blood pressures (Figure 5A) and heart rates (Figure 5B), the hypertensive response to AngII was significantly attenuated in SMKO mice (Figure 5A). In an attempt to explain the blunted hypertensive response to AngII in SMKO, and because it has been reported previously that SirT1 regulates AT1R expression in cultured VSM cells,[25] we analyzed AT1R mRNA levels in aortas and mesenteric arteries by quantitative RT-PCR. At baseline, there was no difference in AT1R mRNA between WT and SMKO; however, AngII increased AT1R mRNA in WT but not in SMKO arteries, suggesting that the lower hypertensive response to AngII in SMKO mice may be due to decreased expression of AT1R (Figure 5C and 5D).

We further characterized the pressure response to other vasoconstrictors using high-fidelity pressure catheters inserted into the carotid artery of anesthetized mice. Baseline mean arterial pressure and the pressure response to an intravenous bolus of phenylephrine (100 μL, 1 mmol/L) were comparable in WT and SMKO littermates (Figure 5E), suggesting that SirT1 deficiency in VSM does not induce a generalized effect on vasopressor responses. Moreover, the dramatic incidence of aortic dissection in SMKO mice given AngII was not a mere consequence of increased hemodynamic load on the aorta because an equipotent dose of norepinephrine (10 mg/kg per day) increased blood pressure to the same extent as did AngII and in WT mice (Figure 5F), as measured by radiotelemetry, but failed to cause aortic dissections in any of SMKO mice (0 of 5).

Structural and Mechanical Changes in SMKO Aorta in Response to AngII

There was no apparent alteration in the number or organization of aortic elastic lamellae in SMKO aortas, excluding a developmental elastin defect in SMKO mice; however, following AngII, SMKO aortas showed disordered elastic lamellae with frequent elastin breaks (Figure 6A) and decreased medial hypertrophy (Table). An assessment of elastin microstructure by multiphoton microscopy[16] at multiple locations along the aorta revealed typical parallel microstructure of elastin fibers in each elastic lamellae in SMKO mice at baseline, similar to WT littermates. After AngII, the elastin fiber network appeared disorganized in SMKO aortas and demonstrated significantly

Table. Lack of VSM SirT1 Prevents AngII-Induced Aortic Hypertrophy

Medial Thickness	Saline	AngII
WT	51.6±1.1 μm	67.0±3.0 μm*
SMKO	51.0±0.2 μm	54.8±3.2 μm†

Medial thickness (in microns) measured in saline- and AngII-treated WT and SMKO aortas: n=8, WT/saline; n=7, SMKO/saline; n=10, WT/AngII; n=7, SMKO/AngII. AngII indicates angiotensin II; SMKO, smooth muscle sirtuin-1 knockout; WT, wild type.
**P*<0.05 vs WT/saline.
†*P*<0.05 vs WT/AngII.

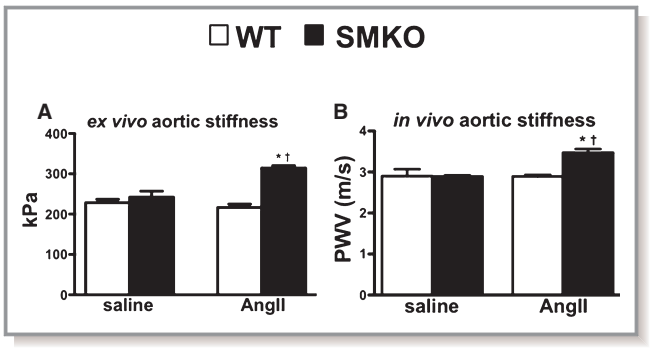

Figure 7. Mechanical properties of SMKO aortas. A, Mechanical ex vivo testing of viable, nondissected aortic rings from saline- or AngII-treated WT and SMKO mice. n=4, WT/saline; n=4, SMKO/saline; n=5, WT/AngII; n=5, SMKO/AngII. B, Aortic stiffness assessed in vivo by PWV, expressed in meters per second. **P*<0.05 vs saline; †*P*<0.05 vs WT/AngII. n=4 in each group. AngII indicates angiotensin II; PWV, pulse wave velocity; SMKO, smooth muscle sirtuin-1 knockout; WT, wild type.

increased dispersion, indicative of fragmentation and disruption (Figure 6B and 6C).

To evaluate the biomechanical properties of the aortic wall in WT and SMKO aortas, with and without AngII, we used an ex vivo measure of arterial stiffness in viable aortic rings from segments of the aorta that had no apparent dissection. Baseline arterial stiffness did not differ between SMKO and WT mice but was significantly increased after 5 days of AngII in SMKO aortas (Figure 7A), as expected in aortas with disorganized elastin.[26] Consistent with ex vivo measurements, pulse wave velocity—an in vivo index of arterial stiffness measured in anesthetized mice at a comparable range of mean arterial pressure—was significantly increased in SMKO mice treated with AngII for 5 days (Figure 7B).

Molecular Mechanisms of Aortic Dissection in AngII-Treated SMKO Mice

To start understanding the molecular mechanisms by which VSM SirT1 deficiency may lead to elastin fragmentation and aortic dissection, we assessed the expression and activity of MMPs, major elastin-degrading enzymes in the extracellular matrix, on isolated aortic extracts after 5 days of AngII, before any deaths occurred. Among various MMPs tested (MMP2, MMP3, MMP9, MMP19), MMP2 and MMP9 mRNA expression in isolated VSM cell extracts were significantly higher in SMKO than WT extracts at baseline. In vitro treatment of VSM cells with AngII (100 nmol/L, 6 hours) increased MMP2 and MMP9 mRNA in both WT and SMKO extracts but to a significantly greater extent in SMKO (Figure 8A). In-gel zymography of whole aortic extracts showed a significant increase in activities of MMP2 and MMP9 in SMKO extracts,

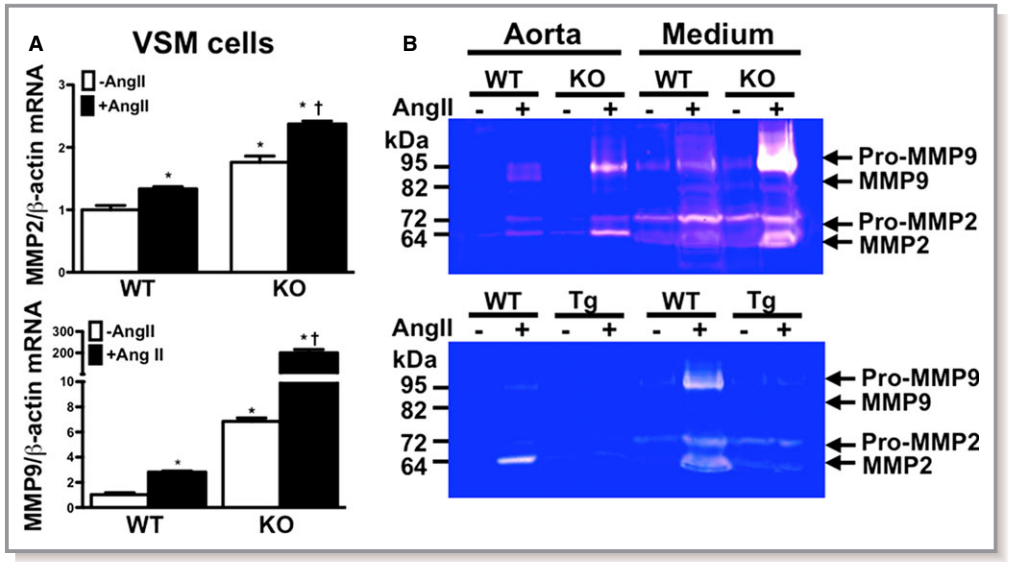

Figure 8. VSM SirT1 prevents MMP activation in the aorta. A, MMP2 and MMP9 mRNA levels assessed by quantitative RT-PCR in cultured VSM cells from WT and SMKO (KO) aortas, with or without AngII (100 nmol/L, 6 hours; n=3 in each group, in duplicate experiments). **P*<0.05 vs no-AngII control; †*P*<0.05 vs WT/AngII. MMP2 and MMP9 mRNA expressed as fold change vs WT/no-AngII control. B, Representative images of in-gel zymography indicative of MMP activities in aortas and their culture medium from saline- or AngII-treated WT and SMKO mice and mice overexpressing SirT1 in VSM (Tg). Each lane represents 1 mouse; n=4 in each group. AngII indicates angiotensin II; kDa, kiloDalton; MMP, matrix metalloproteinase; SMKO, smooth muscle SirT1 knockout; WT, wild type.

particularly when assessed in the medium of cultured aortas (Figure 8B, top panel). Increases in MMP2 and MMP9 did not occur in mice overexpressing SirT1 in VSM (SMTg) (Figure 8B, bottom panel).

Because oxidants play an important role in the response of the aortic wall to AngII and MMP activation, we measured ROS on freshly frozen aortic sections, which indicated greater oxidant production in aortas of AngII-treated SMKO mice compared with AngII-treated WT mice (Figure 9A and quantitation in graph). Similarly, lack of SirT1 in VSM enhanced AngII-induced oxidant production in cultured VSM cells, as assessed by flow cytometry (Figure 9B). Incubation of cultured aortas with tempol (10 mmol/L), an oxidant scavenger, completely prevented AngII-induced MMP activation (Figure 9C).

Tissue inhibitor of metalloproteinase-1 (TIMP-1) is an endogenous inhibitor of MMP activity and is regulated by SirT1 in lung fibroblasts.[27] TIMP-1 expression was impaired in

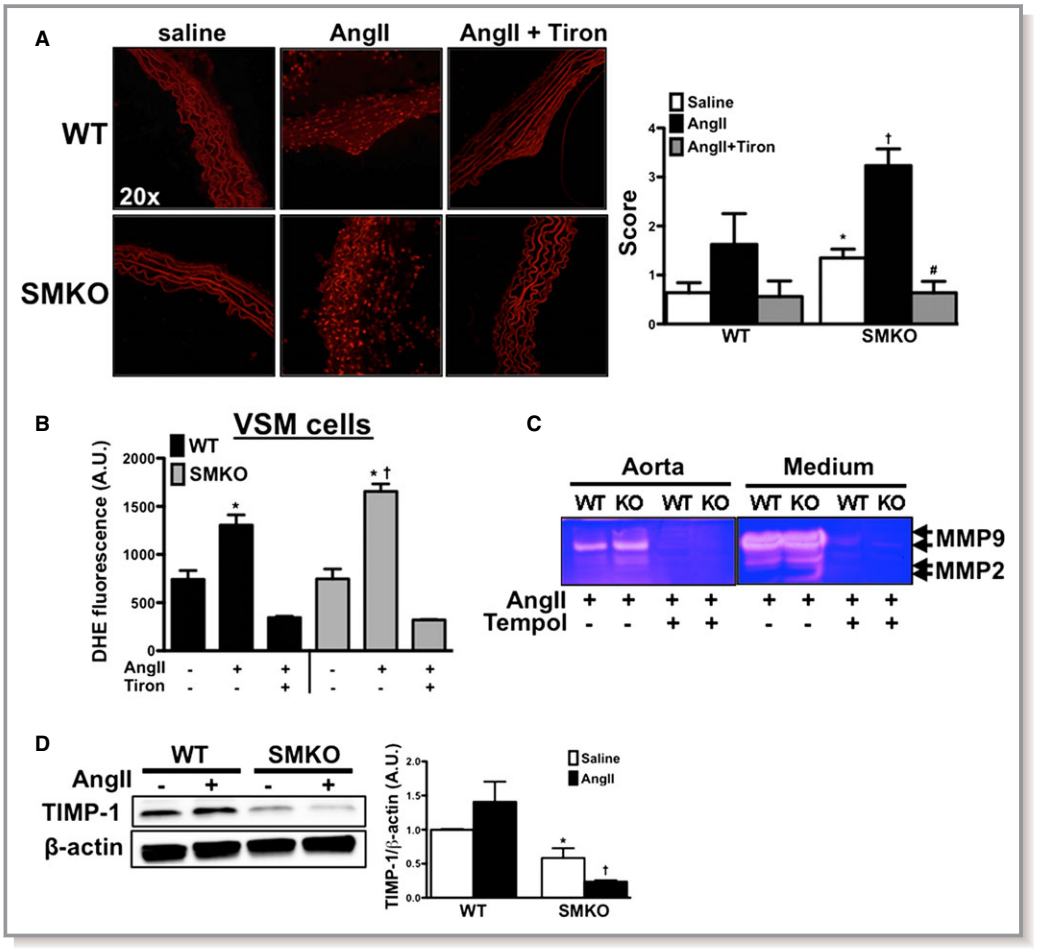

Figure 9. AngII-stimulated oxidant production in SMKO aortas and VSM cells is responsible for MMP activation. A, Representative pictures of DHE-stained aortic sections from WT and SMKO mice 3 days after AngII infusion (n=7, WT/saline; n=5, SMKO/saline; n=5, WT/AngII; n=12, SMKO/AngII), quantified in graph. **P*<0.05 vs WT/saline; †*P*<0.05 vs WT/AngII, #*P*<0.05 vs SMKO/AngII. B, Oxidant production, mainly superoxide, detected by DHE fluorescence and flow cytometry in cultured VSM cells from WT and SMKO mice and treated with AngII. n=3 in each group, in duplicate experiments; **P*<0.05 vs WT/no AngII; †*P*<0.05 vs WT/AngII. Tiron (10 mmol/L), a superoxide scavenger, was used to demonstrate specificity of DHE fluorescence in both cells and aortic sections. C, The oxidant scavenger tempol (10 mmol/L) prevents AngII-stimulated MMP activation in cultured aorta, measured by in-gel zymography; each lane represents 1 mouse in duplicate experiments. D, Representative image of triplicate Western blots for TIMP-1 from aortic homogenates of indicated mice; each lane represents 1 mouse. Band-intensity quantitation, normalized to β-actin, and expressed as arbitrary units (AU) in graph; **P*<0.05 vs WT/no AngII; †*P*<0.05 vs WT/AngII. AngII indicates angiotensin II; DHE, dihydroethidine; KO or SMKO, smooth muscle SirT1 knockout; MMP, matrix metalloproteinases; TIMP-1, tissue inhibitor of metalloproteinase-1; VSM, vascular smooth muscle; WT, wild type.

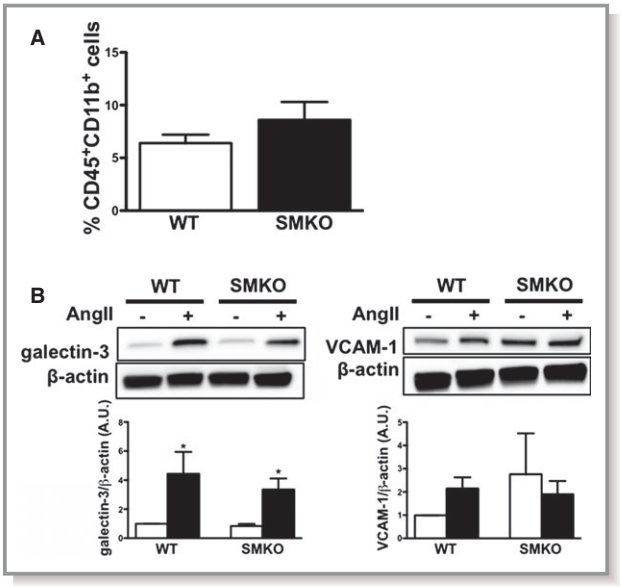

Figure 10. Inflammatory cell infiltration in the aorta after AngII. A, % $CD45^+CD11b^+$ cells in aortic homogenates from WT (n=5) and SMKO (n=4) mice after 5 days of AngII treatment, quantified by flow cytometry. B, Representative Western blot for galectin-3, a marker of activated macrophages, and the adhesion molecule VCAM-1 in aortic homogenates. Each lane represents 1 mouse in triplicate Western blots. Quantitation of band intensities is expressed in arbitrary units (AU) in graphs. **P*<0.05 vs saline. AngII indicates angiotensin II; SMKO, smooth muscle sirtuin-1 knockout; WT, wild type.

SMKO aortas in both saline- and AngII-treated mice compared with WT aortas (Figure 9D and quantitation in graph).

Inflammatory cells that are resident or recruited in the aortic wall in response to AngII may contribute to increased oxidant production and MMP activity, leading to aortic dissection. After 5 days of AngII, SMKO aortas had numbers of $CD45^+CD11b^+$ cells, assessed by flow cytometry (Figure 10A), and expression of the macrophage marker galectin-3 and the adhesion molecule VCAM-1 (Figure 10B) comparable to WT littermates.

Discussion

SirT1 is an evolutionarily conserved enzyme that deacetylates multiple intracellular targets and is important for a variety of cellular functions such as DNA damage repair, cell cycle regulation, apoptosis, senescence, and adaptation to metabolic stress. In the present study, we investigated the role of endogenous SirT1 in VSM during AngII infusion, using a novel mouse model lacking functional SirT1 in VSM (SMKO). We found that aortas lacking SirT1 in smooth muscle cells, although structurally and functionally not different from WT littermates at baseline, were prone to aortic dissections after modest doses of AngII (1 mg/kg per day), with only 30% of SMKO mice surviving a 14-day AngII treatment. In SMKO mice, blood pressures at baseline and after α-adrenergic agonists were not different than those in WT mice, indicating that lack of SirT1 in VSM does not affect peripheral vascular resistance or α-adrenergic vasoconstriction responses. Nonetheless, after even brief exposure to AngII (5 days), 42% (24 of 56) of the SMKO mice were alive but with dissected aortas. This was associated with increased oxidant production and MMP activities, leading to severe elastin fragmentation compared with WT. Our findings strongly implicate a requirement of the aortic wall for VSM SirT1 to maintain structural and functional integrity and to prevent aortic dissection by preventing matrix metalloproteinase activation and elastin fragmentation.

Notably, AngII-induced aortic dissections in SMKO mice were not a mere consequence of increased hemodynamic stress on the aortic wall because (1) AngII-induced hypertension was blunted in SMKO mice compared with WT mice and (2) a hypertensive dose of norepinephrine—a vasoconstrictor that, compared with AngII, does not induce inflammation and oxidant production in the vasculature[28]—did not cause aortic dissections despite systolic blood pressure increases similar to those caused by AngII in the SMKO mice. A blunted hypertensive response of SMKO mice to AngII appears to be due to a failure of SMKO arteries to upregulate AT1R in response to AngII infusion (Figure 5C and 5D). A recent study demonstrated involvement of SirT1 in AT1R promoter regulation using cultured VSM cells,[25] but the mechanisms by which SirT1 regulates AT1R in vivo warrant further investigation.

In our study, MMP activation in response to AngII was prevented in mice overexpressing SirT1 in VSM, pointing to MMP as a VSM SirT1 downstream target and the cause of elastolysis and aortic dissection. SirT1 negatively regulates MMP gene transcription and activity via multiple mechanisms, namely, by deacetylating nuclear factor κB[29,30] and TIMP-1,[27] an endogenous MMP antagonist. Both saline- and AngII-treated aortas of SMKO mice had significantly lower TIMP-1 protein expression compared with WT mice (Figure 9D). In addition, MMPs are posttranscriptionally activated by ROS, mainly by glutathionylation of cysteine residues in the active site.[31] SirT1 deficiency in VSM was associated with increased ROS production, as assessed in AngII-treated SMKO VSM cells and aortic sections (Figure 9A and 9B). This is consistent with the fact that SirT1 boosts the cellular antioxidant capacity by directly stimulating nuclear factor E2-related factor 2,[32] a transcription factor that induces the expression of 2 potent oxidant-scavenging enzymes (hemoxygenase-1 and superoxide dismutase), and by modulating FOXO and p66shc.[8,33] To the extent that MMPs are activated by ROS, excessive ROS on AngII infusion and in settings of SirT1 deficiency might also have contributed to MMP activation in

SMKO aortas, as corroborated by the fact that tempol (an oxidant scavenger) was able to completely prevent AngII-induced MMP activation (Figure 9C). Notably, although structurally normal at baseline, SMKO aortas are primed for activation of MMPs, as indicated by an increase in baseline MMP mRNA expression and oxidants. It is likely that SirT1 regulates multiple factors responsible for alterations in MMP mRNA and protein expression, oxidant production, and scavenging and for MMP activity responsible for elastin breakdown, increased stiffness, and dissection of the aorta, despite lower blood pressure.

Considering that activation and infiltration of inflammatory cells in the aorta is a hallmark of this model of AngII hypertension,[34] we cannot exclude a contribution of inflammatory cells to oxidant production and MMP activation in aortas of AngII-treated mice; however, our study indicated that the exaggerated oxidant production and MMP activities in SMKO aortas leading to aortic dissection are not due to increased recruitment of inflammatory cells in aortas lacking VSM SirT1 compared with WT aortas after AngII.

Aortic dissection is a life-threatening condition for which treatment options are currently limited. Our study demonstrates that VSM SirT1 is a crucial requirement for vessel integrity and for preventing aortic dissection in settings of AngII hypertension. Of note, a recent study used the same VSM SirT1 knockout mice as ours and reported that the mice, when on an apolipoprotein E–null background and fed an atherogenic diet, were prone to atherosclerotic plaque formation to a greater extent than controls. Interestingly, in 2 of 12 mice studied, medial degeneration and elastin fragmentation were evident in atherosclerotic lesions and associated with aortic aneurysm and dissection.[10] Although the authors underscored that these pathological features were observed only in 16% of mice with apolipoprotein E deletion and concomitant fat feeding but not in controls, their data pointed to a broader protective role of VSM SirT1 against aortic media tearing and dissection. Furthermore, resveratrol, a natural polyphenol known to activate SirT1, has recently been shown to prevent arterial remodeling and stiffening in mice[35,36] and in nonhuman primates.[37] Consequently, polyphenols and specific SirT1 activators could be attractive therapeutic approaches against aortic dissections or rupture in patients at risk, such as hypertensive persons or those with Marfan's syndrome and related disorders.

Acknowledgments

We would like to thank Dr Josenia Tan in the Boston University School of Medicine Department of Pathology for the pathological evaluation of aortic sections, and Dr Charles P. Lin from the Advanced Microscopy Program, Center for Systems Biology and Wellman Center for Photomedicine, Massachusetts General Hospital/Harvard Medical School, for providing access to the multiphoton microscope. We also thank the laboratory of Dr David Sinclair that provided the SirT1 floxed mice backcrossed onto to C57BL6 genetic background.

Sources of Funding

This work was supported by NHLBI R01 grant HL105287 to Cohen and was partially supported by a grant from Servier Research Institute (Suresnes, France), the Evans Center for Interdisciplinary Biomedical Research ARC at Boston University (http://www.bumc.bu.edu/evanscenteribr/), NHLBI R01 grant HL098028 to Zhang, Ruth Kirschstein Postdoctoral Fellowship T32 HL07224 at the Whitaker Cardiovascular Institute Multidisciplinary Training Program to Fry and The Marfan's Foundation Early Investigator grant to Seta.

Disclosures

None.

References

1. Wang HD, Xu S, Johns DG, Du Y, Quinn MT, Cayatte AJ, Cohen RA. Role of NADPH oxidase in the vascular hypertrophic and oxidative stress response to angiotensin II in mice. *Circ Res*. 2001;88:947–953.
2. Fleenor BS, Marshall KD, Durrant JR, Lesniewski LA, Seals DR. Arterial stiffening with ageing is associated with transforming growth factor-beta1-related changes in adventitial collagen: reversal by aerobic exercise. *J Physiol*. 2010;588:3971–3982.
3. Wang M, Khazan B, Lakatta EG. Central arterial aging and angiotensin II signaling. *Curr Hypertens Rev*. 2010;6:266–281.
4. Fan LM, Douglas G, Bendall JK, McNeill E, Crabtree MJ, Hale AB, Mai A, Li JM, McAteer MA, Schneider JE, Choudhury RP, Channon KM. Endothelial cell-specific reactive oxygen species production increases susceptibility to aortic dissection. *Circulation*. 2014;129:2661–2672.
5. Cohen HY, Miller C, Bitterman KJ, Wall NR, Hekking B, Kessler B, Howitz KT, Gorospe M, de Cabo R, Sinclair DA. Calorie restriction promotes mammalian cell survival by inducing the SIRT1 deacetylase. *Science*. 2004;305:390–392.
6. Haigis MC, Sinclair DA. Mammalian sirtuins: biological insights and disease relevance. *Annu Rev Pathol*. 2010;5:253–295.
7. Kawai Y, Garduno L, Theodore M, Yang J, Arinze IJ. Acetylation-deacetylation of the transcription factor Nrf2 (nuclear factor erythroid 2-related factor 2) regulates its transcriptional activity and nucleocytoplasmic localization. *J Biol Chem*. 2011;286:7629–7640.
8. Zhou S, Chen HZ, Wan YZ, Zhang QJ, Wei YS, Huang S, Liu JJ, Lu YB, Zhang ZQ, Yang RF, Zhang R, Cai H, Liu DP, Liang CC. Repression of P66Shc expression by SIRT1 contributes to the prevention of hyperglycemia-induced endothelial dysfunction. *Circ Res*. 2011;109:639–648.
9. Yeung F, Hoberg JE, Ramsey CS, Keller MD, Jones DR, Frye RA, Mayo MW. Modulation of NF-kappaB-dependent transcription and cell survival by the SIRT1 deacetylase. *EMBO J*. 2004;23:2369–2380.
10. Gorenne I, Kumar S, Gray K, Figg N, Yu H, Mercer J, Bennett M. Vascular smooth muscle cell sirtuin 1 protects against DNA damage and inhibits atherosclerosis. *Circulation*. 2013;127:386–396.
11. Li L, Zhang HN, Chen HZ, Gao P, Zhu LH, Li HL, Lv X, Zhang QJ, Zhang R, Wang Z, She ZG, Wei YS, Du GH, Liu DP, Liang CC. SIRT1 acts as a modulator of neointima formation following vascular injury in mice. *Circ Res*. 2011;108:1180–1189.
12. Gao P, Xu TT, Lu J, Li L, Xu J, Hao DL, Chen HZ, Liu DP. Overexpression of SIRT1 in vascular smooth muscle cells attenuates angiotensin II-induced vascular remodeling and hypertension in mice. *J Mol Med (Berl)*. 2014;92:347–357.
13. Gao YZ, Saphirstein RJ, Yamin R, Suki B, Morgan KG. Aging impairs smooth muscle-mediated regulation of aortic stiffness: a defect in shock absorption function? *Am J Physiol Heart Circ Physiol*. 2014;307:H1252–H1261.

14. Zoumi A, Lu X, Kassab GS, Tromberg BJ. Imaging coronary artery microstructure using second-harmonic and two-photon fluorescence microscopy. *Biophys J*. 2004;87:2778–2786.
15. Boulesteix T, Pena AM, Pages N, Godeau G, Sauviat MP, Beaurepaire E, Schanne-Klein MC. Micrometer scale ex vivo multiphoton imaging of unstained arterial wall structure. *Cytometry A*. 2006;69:20–26.
16. Chow MJ, Turcotte R, Lin CP, Zhang Y. Arterial extracellular matrix: a mechanobiological study of the contributions and interactions of elastin and collagen. *Biophys J*. 2014;106:2684–2692.
17. Liu ZQ. Scale space approach to directional analysis of images. *Appl Opt*. 1991;30:1369–1373.
18. Turcotte R, Alt C, Mortensen LJ, Lin CP. Characterization of multiphoton microscopy in the bone marrow following intravital laser osteotomy. *Biomed Opt Express*. 2014;5:3578–3588.
19. Qin Z, Hou X, Weisbrod RM, Seta F, Cohen RA, Tong X. Nox2 mediates high fat high sucrose diet-induced nitric oxide dysfunction and inflammation in aortic smooth muscle cells. *J Mol Cell Cardiol*. 2014;72:56–63.
20. Moore JP, Sakkal S, Bullen ML, Kemp-Harper BK, Ricardo SD, Sobey CG, Drummond GR. A flow cytometric method for the analysis of macrophages in the vascular wall. *J Immunol Methods*. 2013;396:33–43.
21. Cheng HL, Mostoslavsky R, Saito S, Manis JP, Gu Y, Patel P, Bronson R, Appella E, Alt FW, Chua KF. Developmental defects and p53 hyperacetylation in Sir2 homolog (SIRT1)-deficient mice. *Proc Natl Acad Sci USA*. 2003;100:10794–10799.
22. Potente M, Ghaeni L, Baldessari D, Mostoslavsky R, Rossig L, Dequiedt F, Haendeler J, Mione M, Dejana E, Alt FW, Zeiher AM, Dimmeler S. SIRT1 controls endothelial angiogenic functions during vascular growth. *Genes Dev*. 2007;21:2644–2658.
23. Li L, Miano JM, Cserjesi P, Olson EN. SM22 alpha, a marker of adult smooth muscle, is expressed in multiple myogenic lineages during embryogenesis. *Circ Res*. 1996;78:188–195.
24. Goldfinger JZ, Halperin JL, Marin ML, Stewart AS, Eagle KA, Fuster V. Thoracic aortic aneurysm and dissection. *J Am Coll Cardiol*. 2014;64:1725–1739.
25. Miyazaki R, Ichiki T, Hashimoto T, Inanaga K, Imayama I, Sadoshima J, Sunagawa K. SIRT1, a longevity gene, downregulates angiotensin II type 1 receptor expression in vascular smooth muscle cells. *Arterioscler Thromb Vasc Biol*. 2008;28:1263–1269.
26. Wagenseil JE, Mecham RP. Elastin in large artery stiffness and hypertension. *J Cardiovasc Transl Res*. 2012;5:264–273.
27. Yao H, Hwang JW, Sundar IK, Friedman AE, McBurney MW, Guarente L, Gu W, Kinnula VL, Rahman I. SIRT1 redresses the imbalance of tissue inhibitor of matrix metalloproteinase-1 and matrix metalloproteinase-9 in the development of mouse emphysema and human COPD. *Am J Physiol Lung Cell Mol Physiol*. 2013;305:L615–L624.
28. Rajagopalan S, Kurz S, Munzel T, Tarpey M, Freeman BA, Griendling KK, Harrison DG. Angiotensin II-mediated hypertension in the rat increases vascular superoxide production via membrane NADH/NADPH oxidase activation. Contribution to alterations of vasomotor tone. *J Clin Invest*. 1996;97:1916–1923.
29. Nakamaru Y, Vuppusetty C, Wada H, Milne JC, Ito M, Rossios C, Elliot M, Hogg J, Kharitonov S, Goto H, Bemis JE, Elliott P, Barnes PJ, Ito K. A protein deacetylase SIRT1 is a negative regulator of metalloproteinase-9. *FASEB J*. 2009;23:2810–2819.
30. Kowluru RA, Santos JM, Zhong Q. Sirt1, a negative regulator of matrix metalloproteinase-9 in diabetic retinopathy. *Invest Ophthalmol Vis Sci*. 2014;55:5653–5660.
31. Kandasamy AD, Chow AK, Ali MA, Schulz R. Matrix metalloproteinase-2 and myocardial oxidative stress injury: beyond the matrix. *Cardiovasc Res*. 2010;85:413–423.
32. Huang K, Huang J, Xie X, Wang S, Chen C, Shen X, Liu P, Huang H. Sirt1 resists advanced glycation end products-induced expressions of fibronectin and TGF-beta1 by activating the Nrf2/ARE pathway in glomerular mesangial cells. *Free Radic Biol Med*. 2013;65:528–540.
33. Webster BR, Lu Z, Sack MN, Scott I. The role of sirtuins in modulating redox stressors. *Free Radic Biol Med*. 2012;52:281–290.
34. Barhoumi T, Kasal DA, Li MW, Shbat L, Laurant P, Neves MF, Paradis P, Schiffrin EL. T regulatory lymphocytes prevent angiotensin II-induced hypertension and vascular injury. *Hypertension*. 2011;57:469–476.
35. Baur JA, Pearson KJ, Price NL, Jamieson HA, Lerin C, Kalra A, Prabhu VV, Allard JS, Lopez-Lluch G, Lewis K, Pistell PJ, Poosala S, Becker KG, Boss O, Gwinn D, Wang M, Ramaswamy S, Fishbein KW, Spencer RG, Lakatta EG, Le Couteur D, Shaw RJ, Navas P, Puigserver P, Ingram DK, de Cabo R, Sinclair DA. Resveratrol improves health and survival of mice on a high-calorie diet. *Nature*. 2006;444:337–342.
36. Pearson KJ, Baur JA, Lewis KN, Peshkin L, Price NL, Labinskyy N, Swindell WR, Kamara D, Minor RK, Perez E, Jamieson HA, Zhang Y, Dunn SR, Sharma K, Pleshko N, Woollett LA, Csiszar A, Ikeno Y, Le Couteur D, Elliott PJ, Becker KG, Navas P, Ingram DK, Wolf NS, Ungvari Z, Sinclair DA, de Cabo R. Resveratrol delays age-related deterioration and mimics transcriptional aspects of dietary restriction without extending life span. *Cell Metab*. 2008;8:157–168.
37. Mattison JA, Wang M, Bernier M, Zhang J, Park SS, Maudsley S, An SS, Santhanam L, Martin B, Faulkner S, Morrell C, Baur JA, Peshkin L, Sosnowska D, Csiszar A, Herbert RL, Tilmont EM, Ungvari Z, Pearson KJ, Lakatta EG, de Cabo R. Resveratrol prevents high fat/sucrose diet-induced central arterial wall inflammation and stiffening in nonhuman primates. *Cell Metab*. 2014;20:183–190.